Cardiomyocyte-specific knockdown of *Hmgcs2* improved cardiac utilization of fatty acids, β-hydroxybutyrate, and glucose in T2DM mice through suppression of cardiac ketogenesis. This intervention, coupled with a reduction in circulating β-hydroxybutyrate levels, attenuated diabetes-associated AF.
Conclusion: Myocardial Hmgcs2-driven ketogenesis contributes to systemic hyperketonemia and promotes atrial arrhythmogenesis in T2DM, identifying Hmgcs2 as a potential therapeutic target for diabetic AF and heart failure with preserved ejection fraction (HFpEF).

PO-02-288

ADVANCED AGE PROMOTES ATRIAL ECTOPY AND ATRIAL FIBRILLATION STABILIZATION: THE ROLE OF ACTIVATED COAGULATION FACTORS AND THE ATRIAL INFLAMMASOME

Elisa D'Alessandro; Billy Scaf; Pascal Martsch; Arne Van Hunnik; Issam Abu Taha; Vladimir Sobota; Marion Kuiper; Rene van Oerle; Henri Spronk; Frans van Nieuwenhoven; Hugo ten Cate; Sander Verheule; Dobromir Dobrev and Ulrich Schotten

Background: Age is a risk factor for atrial fibrillation (AF) and for stroke in patients with AF. Activated coagulation factors and their receptors (PARs) can promote NLRP3 inflammasome activation, which is involved in the pathogenesis of AF.
Objective: To investigate the effect of aging on atrial ectopy, AF substrate development, and AF stabilisation, as well as AF-mediated activation of coagulation factors and the atrial inflammasome.
Methods: Four groups of goats were studied: Young (<3 years) sinus rhythm (Y-SR, n=9), Young AF (Y-AF n=7), Old (>8 years) sinus rhythm (O-SR, n=6), and Old AF (O-AF, n=8). Atrial ectopy and AF stabilisation were monitored during 4 weeks of atrial burst pacing. Clotting potential was measured using thrombin generation assays at baseline and 4 weeks (final). Hemodynamics and AF characteristics were assessed at the final experiment. Atrial samples were collected for histological, gene and protein expression analyses.
Results: Old goats exhibited faster AF stabilization (179 ± 374 vs.1487 ± 614 AF paroxysms) and more frequent premature atrial contractions (~ 4-fold increase) compared to young goats, but no increased AF complexity. Old goats showed higher constitutive atrial NLRP3 inflammasome activity (Casp1-p20: ~1.8-fold increase, GSDMD-NT: ~1.7-fold increase, and IL-1β: ~2.7-fold increase) relative to young goats. Thrombin generation did not differ between young and old goats at baseline. Four weeks of AF increased thrombin generation in old (baseline 178.8 ± 35.6 nM vs. final 219.5 ± 52.2 nM), but not in young goats. In old goats, AF elicited atrial myocyte hypertrophy (O-AF: 13.79 μm [95% CI: 13.06, 14.53] vs. O-SR: 12.17 μm [95% CI: 11.32, 13.02]) and left atrial epicardial endomysial fibrosis (cell to cell distance, O-AF: 3.15 μm [95% CI: 2.83, 3.47] vs. O-SR: 2.91 μm [95% CI: 2.59, 3.24], along with increased atrial pro-fibrotic (COL1A1: ~8.9-fold increase) and pro-hypertrophic (NPPA: ~2.9-fold increase, NPPB: ~12.9-fold increase) gene expression, compared to age-matched controls.
Conclusion: Age accelerates AF stabilization, possibly through enhanced atrial ectopy and faster development of conduction alterations compared to young goats. In old goats, AF susceptibility was accompanied by elevated baseline activation of the atrial NLRP3 inflammasome, which may have contributed to enhanced atrial ectopy and conduction disturbances. In older animals, AF increased thrombin generation, which may have accelerated the development of a structural substrate for AF.

PO-02-289

SILK FIBROIN–INDUCED BIOLOGICAL PACEMAKER ENABLES DEVICE-FREE RHYTHM SUPPORT IN A PORCINE COMPLETE HEART BLOCK MODEL

Chih-Min Liu; Ching-Hui Weng; Pei-Chun Chou; Peng-Chin Tsai; Tzu-Hao Cheng and Yu-Feng Hu

Background: Electronic pacemakers effectively treat bradyarrhythmias but are limited by risks of infection, hardware complications, and lack of physiological autonomic responsiveness. Biological pacemakers are a potential alternative. Silk fibroin (SF) hydrogel has been shown to generate biological pacemaker activity in rodent models, but it remains unknown whether SF can induce physiologically competent, device-free pacing in large animals with clinically relevant syncope.
Objective: To determine whether intracardiac SF hydrogel can generate a biological pacemaker capable of maintaining rhythm without an electronic device.
Methods: A porcine complete heart block model with syncope was established. SF hydrogel was injected into the interventricular septum under intracardiac echocardiography guidance. Electrophysiologic function, autonomic responsiveness, pacing sufficiency, and syncope prevention were evaluated using continuous ECG patch monitoring under conditions with and without electronic backup pacing. Continuous video surveillance assessed behavioral activity. Pacemaker-like cells at the injection site were identified by Hcn4 in situ hybridization.
Results: SF hydrogel induced robust biological pacemaker activity, reducing reliance on electronic pacing to <1% between days 4 and 10 post-injection. Continuous ECG monitoring showed that SF-treated pigs maintained higher mean and maximal heart rates with preserved autonomic responses and diurnal variation compared with controls. Corrected recovery times were significantly shorter in SF-treated animals. Untreated controls exhibited recurrent syncope, whereas SF-treated pigs showed complete prevention of syncope. Pacemaker activity originated near the SF injection site, where Hcn4-positive pacemaker-like cells were detected. Pigs supported solely by SF pacing, without any electronic backup, maintained physiologically appropriate heart rates sufficient for normal daily activities for up to 4 weeks.
Conclusion: SF hydrogel generates a physiologically competent biological pacemaker that prevents syncope in a large-animal heart block model. This approach may offer a viable temporary, device-free pacing strategy for high-risk or hardware-limited clinical settings.

PO-02-290

DEVELOPMENT AND VALIDATION OF A NEW LARGE LANGUAGE MODEL FOR DETECTING ATRIAL FIBRILLATION

Seewon Choi; Mayank Keoliya; Alaia Solko-Breslin; Neelay Velingker; Alireza Oraii; Rajeev Alur; Rajat Deo; Sameed Ahmed Khatana; Mayur Naik and Eric Wong

Background: AI-guided ECG evaluation using deep leaning and convolutional neural networks (CNN) has been used to classify, detect, and predict atrial fibrillation (AF). In addition, large language models (LLM) that interpret ECG images have demonstrated relatively poor performance compared to CNN-based modeling.
Objective: We sought to develop a waveform-based LLM that accepts standard 12-lead ECGs using raw data. We compared its performance to an existing image-based LLM (LLM PULSE)

and the GE 12SL algorithm commonly utilized in the clinical settings to diagnose AF from 12-lead ECGs.
Methods: We designed a specialized encoder that enables the LLM to accept ECG directly as raw values and process them as tokens (Figure 1). Our LLM (LLM Penn) was trained on 1.2 million, publicly available 12-lead ECGs and their diagnostic labels obtained from 412,639 patients across hospitals in US, Brazil, and Germany. External validation was then assessed in 7,154 patients from 16 hospitals worldwide in the zero-shot setting. We compared the diagnostic accuracy of LLM Penn with LLM PULSE and the GE 12SL algorithm. Next, we evaluated LLM Penn on 1,121, single lead, in-hospital telemetry recordings (Icentia dataset). We compared diagnostic metrics for classifying AF across single lead rhythm strips ranging in duration from 10 seconds to 10 minutes.
Results: In external validation, LLM Penn had better sensitivity in classifying AF than either LLM PULSE or the GE 12 SL algorithm (Table 1A). All models had high specificity. In the single lead telemetry analysis, the sensitivity for classifying AF increased as the recording duration increased from 10 to 60 seconds (Table 1B). After 60 seconds, there were only modest improvements in diagnostic metrics.
Conclusion: We developed an LLM that has improved sensitivity in detecting AF compared to the GE algorithm. Also, a minimum of 1-minute telemetry recording leads to enhanced accuracy for AF detection.

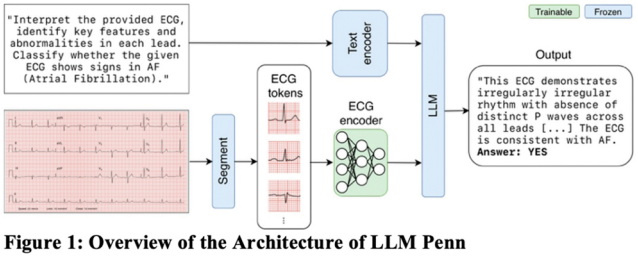

Figure 1: Overview of the Architecture of LLM Penn

Table 1: Diagnostic Metrics for Classifying Atrial Fibrillation

A. Assessment of Standard, 12-lead ECGs

Model	Sensitivity	Specificity	PPV	NPV
LLM Penn	0.93	0.96	0.78	0.99
LLM PULSE	0.60	0.95	0.66	0.94
GE 12 SL	0.76	0.99	0.85	0.99

B. Assessment of LLM Penn across 1-lead telemetry strips of various duration

Duration	Sensitivity	Specificity	PPV	NPV
10 seconds	0.70	0.89	0.45	0.96
30 seconds	0.74	0.96	0.71	0.97
60 seconds	0.80	0.96	0.72	0.98
2 minutes	0.79	0.97	0.79	0.98
5 minutes	0.81	0.98	0.80	0.98
10 minutes	0.84	0.97	0.76	0.98

PO-02-291

NOVEL MECHANISMS UNDERLYING PRO-INFLAMMATORY CYTOKINE IL17A-TRIGGERED ARRHYTHMOGENESIS

Aaryan Kohli; Saugat Khanal; Nikola Ricchiuti; Jiajie Yan; Xiaoping Wan; Isabelle Deschenes; Dan J. Bare and Xun Ai

Background: Inflammation increases the risk of AF and ventricular arrythmias. The mechanisms are complex and far from being understood, and clinical strategies of suppressing single cytokines produce limited benefits, even worsening disease condition. The pro-inflammatory cytokine interleukin-17 (IL17), including IL17A, IL17F, and heterodimer IL17A/F, has been implicated in cardiovascular diseases, but its role in arrhythmia remains unclear. We previously identified stress kinase JNK2 as a driver of arrhythmias through promoting sarcoplasmic reticulum (SR) Ca^{2+}-triggered arrhythmic activities. The link between IL17 and JNK2 in inflammation-associated arrhythmias remains unclear.
Objective: To determine the arrhythmic potential of IL-17 and its relationship with pro-arrhythmic kinase JNK2.
Methods: Adult rabbit atrial and ventricular myocytes were treated with IL17A, IL17F, IL17A/F (5 ng/mL; 16-24 hrs), or TNFα (25ng/mL). Our well-validated JNK2-inhibitor (JNK2i; 40 nM) or TNFα blocker R7050 (1.5 μM) were applied 1 h prior. Tetracaine-sensitive SR Ca^{2+} leak and pacing-induced delayed-after-depolarization (DADs) were measured using confocal Ca^{2+} imaging and whole-cell patch clamp. JNK phosphorylation was assessed by immunoblotting. An established systemic inflammation model of Dextran Sodium Sulfate (DSS) mice was also used, and AF inducibility and biochemistry assays were conducted using our optimized protocols.
Results: IL17A significantly increased SR Ca^{2+} leak and DAD incidence in both ventricular and atrial myocytes ($p<0.001$), while JNK2i attenuated these effects ($p<0.01$). IL17A increased JNK-phosphorylation, reversed by JNK2i ($p<0.01$), suggesting a key role of JNK2 in IL17-evoked arrhythmogenicity. Intriguingly, IL17A/F, but not IL17F alone, produced $\sim$50% of the IL17A response ($p<0.001$), identifying IL17A as the dominant arrhythmogenic form. We recently established that TNFα-activated JNK2, driving diastolic SR Ca^{2+} leak. IL17A-evoked Ca^{2+} leak was also abolished by R7050 ($p<0.01$), suggesting IL17A interplays with the TNFα-JNK2 axis. DSS mice showed elevated circulating IL17A accompanied by increased cardiac TNFα and JNK2 activation, which enhanced AF susceptibility; this effect was abolished by either JNK2 or TNFα *in vivo* blockage ($p<0.05$), supporting a shared JNK2-dependent mechanism
Conclusion: IL17A promotes SR Ca^{2+} dysregulation through a TNFα-JNK2 pathway, driving AF pathogenesis. Targeting this cytokine-kinase axis may provide a promising strategy to prevent inflammation-associated cardiac arrythmias.

PO-02-292

ENHANCED FAR-FIELD REJECTION AND ACCURATE ACTIVATION TIMING IN FIBROTIC SUBSTRATES USING COAXIAL ELECTROGRAMS

Bram den Ouden; Mark Hoogendijk; Marion Kuiper; Daniel A. Pijnappels; Edward Vigmond; Arne Van Hunnik; Hans Dierkx and Bastiaan Boukens

Background: Accurately identifying local activation times in extracellular electrograms is essential for successful catheter ablation of cardiac arrhythmias. Coaxial electrograms using only three equally distributed local references may be superior to bipolar electrograms for determining local activation in the healthy heart.
Objective: To validate directional independence and far-field rejection capabilities of coaxial compared to bipolar electrograms across multiple wavefront angles and substrates.
Methods: We used a 5x5 cm 2D tissue slab-based cardiac reaction–diffusion model. Local activation was determined in unipolar and coaxial electrograms as dV/dt_(min), and in bipolar electrograms as V_(max) of absolute potential. As golden standard we used the maximum dV/dt of the upstroke of the local action potential. Next, we fabricated multi-electrode sensor grids to compare unipolar and bipolar electrograms against coaxial electrograms based on three or four equally distributed local references. Epicardial electrograms were recorded from three Langendorff-perfused pig hearts using grids with 3, 6, and 9 mm electrode spacing, 0.5 and 1 mm and electrode sizes.